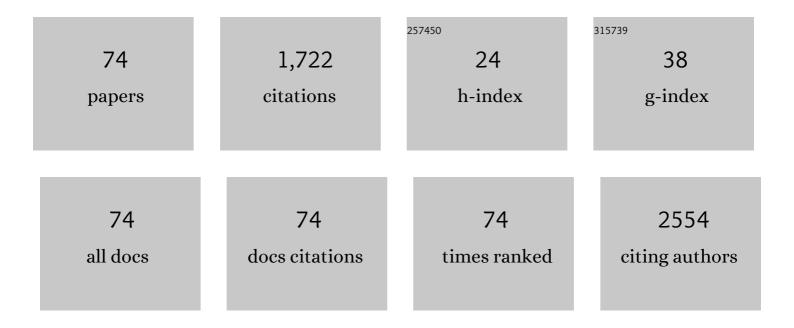
## List of Publications by Year in descending order

Source: https://exaly.com/author-pdf/2497859/publications.pdf Version: 2024-02-01



DAWELLI

#	Article	IF	CITATIONS
1	Intermediates formed during natural attenuation of C9 aromatics under simulated marine conditions: Identification, transformation pathway, and toxicity to microalgae. Environmental Research, 2022, 206, 112558.	7.5	0
2	Characterization, expression, and functional analysis of the pathogenesis-related gene PtDIR11 in transgenic poplar. International Journal of Biological Macromolecules, 2022, 210, 182-195.	7.5	9
3	PSegNet: Simultaneous Semantic and Instance Segmentation for Point Clouds of Plants. Plant Phenomics, 2022, 2022, .	5.9	17
4	Mussel-inspired double cross-linked hydrogels with desirable mechanical properties, strong tissue-adhesiveness, self-healing properties and antibacterial properties. Materials Science and Engineering C, 2021, 120, 111690.	7.3	18
5	Preparation and Characterization of PTFE/PI Nanofiber Composite Assembled Sponges. Fibers and Polymers, 2021, 22, 664-675.	2.1	6
6	A plant-inspired long-lasting adhesive bilayer nanocomposite hydrogel based on redox-active Ag/Tannic acid-Cellulose nanofibers. Carbohydrate Polymers, 2021, 255, 117508.	10.2	77
7	Genome-Wide Characterization of Dirigent Proteins in Populus: Gene Expression Variation and Expression Pattern in Response to Marssonina brunnea and Phytohormones. Forests, 2021, 12, 507.	2.1	9
8	Genome-Wide and Comprehensive Analysis of the Multiple Stress-Related CAF1 (CCR4-Associated Factor) Tj ETQ	q0 <u>3</u> 0 rgE	BT /Overlock
9	Plant Secondary Metabolites with an Overview of Populus. International Journal of Molecular Sciences, 2021, 22, 6890.	4.1	19
10	The preparation of electrospun PVDF/TBAC multi morphology nanofiber membrane and its application in direct contact membrane distillation. Macromolecular Rapid Communications, 2021, , 2100286.	3.9	4
11	Preparation of Centella asiatica loaded gelatin/chitosan/nonwoven fabric composite hydrogel wound dressing with antibacterial property. International Journal of Biological Macromolecules, 2021, 192, 350-359.	7.5	23
12	Development of a DNAzyme-based colorimetric biosensor assay for dual detection of Cd2+ and Hg2+. Analytical and Bioanalytical Chemistry, 2021, 413, 7081-7091.	3.7	12
13	Natural attenuation characteristics and comprehensive toxicity changes of C9 aromatics under simulated marine conditions. Journal of Environmental Sciences, 2021, 109, 26-35.	6.1	9
14	Genome-Wide Evolution and Comparative Analysis of Superoxide Dismutase Gene Family in Cucurbitaceae and Expression Analysis of Lagenaria siceraria Under Multiple Abiotic Stresses. Frontiers in Genetics, 2021, 12, 784878.	2.3	6

15	Identification and Characterization of an OSH1 Thiol Reductase from Populus trichocarpa. Cells, 2020, 9, 76.	4.1	8
16	Isotope Constraints on the Sources of Particulate Organic Carbon in a Subtropical Deep Reservoir. Journal of Geophysical Research G: Biogeosciences, 2020, 125, e2019JG005240.	3.0	2
17	Overexpression of PtDefensin enhances resistance to Septotis populiperda in transgenic poplar. Plant Science, 2020, 292, 110379.	3.6	10

18	Electrospun MnCo2O4/C composite nanofibers as anodes with improved lithium storage performance. Ionics, 2020, 26, 1229-1238.	2.4	1

#	Article	IF	CITATIONS
19	A laccase based biosensor on AuNPs-MoS2 modified glassy carbon electrode for catechol detection. Colloids and Surfaces B: Biointerfaces, 2020, 186, 110683.	5.0	58
20	A Dualâ€Mode Wearable Sensor Based on Bacterial Cellulose Reinforced Hydrogels for Highly Sensitive Strain/Pressure Sensing. Advanced Electronic Materials, 2020, 6, 1900934.	5.1	83
21	Fabrication of Multilayered Nanofiber Scaffolds with a Highly Aligned Nanofiber Yarn for Anisotropic Tissue Regeneration. ACS Omega, 2020, 5, 24340-24350.	3.5	24
22	Mechanically-reinforced 3D scaffold constructed by silk nonwoven fabric and silk fibroin sponge. Colloids and Surfaces B: Biointerfaces, 2020, 196, 111361.	5.0	14
23	Effects of Bt-Cry1Ah1 Transgenic Poplar on Target and Non-Target Pests and Their Parasitic Natural Enemy in Field and Laboratory Trials. Forests, 2020, 11, 1255.	2.1	3
24	FeNi alloy nanoparticles embedded in electrospun nitrogen-doped carbon fibers for efficient oxygen evolution reaction. Journal of Colloid and Interface Science, 2020, 578, 805-813.	9.4	33
25	Hierarchical porous nanofibers containing thymol/beta-cyclodextrin: Physico-chemical characterization and potential biomedical applications. Materials Science and Engineering C, 2020, 115, 111155.	7.3	40
26	Insight into light-driven antibacterial cotton fabrics decorated by in situ growth strategy. Journal of Colloid and Interface Science, 2020, 579, 233-242.	9.4	29
27	Asymmetric Synthesis of Axially Chiral Anilides via Organocatalytic Atroposelective N-Acylation. Organic Letters, 2020, 22, 5331-5336.	4.6	31
28	Overexpression of PtAnnexin1 from Populus trichocarpa enhances salt and drought tolerance in transgenic poplars. Tree Genetics and Genomes, 2020, 16, 1.	1.6	4
29	Bimetallic Catalytic Tandem Reaction of Acyclic Enynones: Enantioselective Access to Tetrahydrobenzofuran Derivatives. Organic Letters, 2020, 22, 3551-3556.	4.6	22
30	Strategies to Increase On-Target and Reduce Off-Target Effects of the CRISPR/Cas9 System in Plants. International Journal of Molecular Sciences, 2019, 20, 3719.	4.1	61
31	An Overlapping-Free Leaf Segmentation Method for Plant Point Clouds. IEEE Access, 2019, 7, 129054-129070.	4.2	27
32	Reusable Surface-Modified Bacterial Cellulose Based on Atom Transfer Radical Polymerization Technology with Excellent Catalytic Properties. Nanomaterials, 2019, 9, 1443.	4.1	3
33	Asymmetric Synthesis of Oxaâ€Bridged Oxazocines through a Catalytic Rh <sup>II</sup> /Zn <sup>II</sup> Relay [4+3] Cycloaddition Reaction. Angewandte Chemie, 2019, 131, 18609-18613.	2.0	5
34	Characterization, expression profiling, and functional analysis of a Populus trichocarpa defensin gene and its potential as an anti-Agrobacterium rooting medium additive. Scientific Reports, 2019, 9, 15359.	3.3	9
35	Asymmetric Synthesis of Oxaâ€Bridged Oxazocines through a Catalytic Rh <sup>II</sup> /Zn <sup>II</sup> Relay [4+3] Cycloaddition Reaction. Angewandte Chemie - International Edition, 2019, 58, 18438-18442.	13.8	34
36	Evaluation, characterization, expression profiling, and functional analysis of DXS and DXR genes of Populus trichocarpa. Plant Physiology and Biochemistry, 2019, 142, 94-105.	5.8	30

#	Article	IF	CITATIONS
37	In situ 3D bacterial cellulose/nitrogen-doped graphene oxide quantum dot-based membrane fluorescent probes for aggregation-induced detection of iron ions. Cellulose, 2019, 26, 6073-6086.	4.9	14
38	Facile fabrication and characterization on alginate microfibres with grooved structure via microfluidic spinning. Royal Society Open Science, 2019, 6, 181928.	2.4	20
39	Overexpression of PtDXS Enhances Stress Resistance in Poplars. International Journal of Molecular Sciences, 2019, 20, 1669.	4.1	20
40	Enantioselective Synthesis of 4-Hydroxy-dihydrocoumarins via Catalytic Ring Opening/Cycloaddition of Cyclobutenones. Organic Letters, 2019, 21, 2388-2392.	4.6	16
41	A multifunctional and highly stretchable electronic device based on silver nanowire/wrap yarn composite for a wearable strain sensor and heater. Journal of Materials Chemistry C, 2019, 7, 13468-13476.	5.5	69
42	Characterization and Function of 3-Hydroxy-3-Methylglutaryl-CoA Reductase in Populus trichocarpa: Overexpression of PtHMGR Enhances Terpenoids in Transgenic Poplar. Frontiers in Plant Science, 2019, 10, 1476.	3.6	25
43	Deposition of polytetrafluoroethylene nanoparticles on graphene oxide/polyester fabrics for oil adsorption. Surface Engineering, 2019, 35, 426-434.	2.2	14
44	Free-standing TiO2–SiO2/PANI composite nanofibers for ammonia sensors. Journal of Materials Science: Materials in Electronics, 2018, 29, 3576-3583.	2.2	19
45	Graphene Oxide/Polyester Fabric Composite by Electrostatic Self-Assembly as a New Recyclable Adsorbent for the Removal of Methylene Blue. Fibers and Polymers, 2018, 19, 1726-1734.	2.1	1
46	Supramolecular Gel-Templated In Situ Synthesis and Assembly of CdS Quantum Dots Gels. Nanoscale Research Letters, 2017, 12, 30.	5.7	6
47	Tin nanoparticles embedded in ordered mesoporous carbon as high-performance anode for sodium-ion batteries. Journal of Solid State Electrochemistry, 2017, 21, 1385-1395.	2.5	23
48	Carbonâ€Coated Magnesium Ferrite Nanofibers for Lithiumâ€ŀon Battery Anodes with Enhanced Cycling Performance. Energy Technology, 2017, 5, 1364-1372.	3.8	22
49	Wintersweet Branchâ€Like C/C@SnO <sub>2</sub> /MoS <sub>2</sub> Nanofibers as Highâ€Performance Li and Naâ€Ion Battery Anodes. Particle and Particle Systems Characterization, 2017, 34, 1700295.	2.3	15
50	DMSO concentration estimation from a diffusion model of PAN-based carbon fibers. , 2017, , .		0
51	Sol-Gel Synthesis of Carbon Xerogel-ZnO Composite for Detection of Catechol. Materials, 2016, 9, 282.	2.9	11
52	Preparation of Pd/Bacterial Cellulose Hybrid Nanofibers for Dopamine Detection. Molecules, 2016, 21, 618.	3.8	32
53	Laccase Biosensor Based on Ag-Doped TiO2 Nanoparticles on CuCNFs for the Determination of Hydroquinone. Nano, 2016, 11, 1650132.	1.0	7
54	Preparation of bacterial cellulose/carbon nanotube nanocomposite for biological fuel cell. Fibers and Polymers, 2016, 17, 1858-1865.	2.1	14

#	Article	IF	CITATIONS
55	Preparation of self-clustering highly oriented nanofibers by needleless electrospinning methods. Fibers and Polymers, 2016, 17, 1414-1420.	2.1	11
56	A directional liquid-transfer nonwoven for skin tissue engineering. Journal of Controlled Release, 2015, 213, e18-e19.	9.9	1
57	NiCu Alloy Nanoparticle-Loaded Carbon Nanofibers for Phenolic Biosensor Applications. Sensors, 2015, 15, 29419-29433.	3.8	26
58	Preparation of a graphene-loaded carbon nanofiber composite with enhanced graphitization and conductivity for biosensing applications. RSC Advances, 2015, 5, 30602-30609.	3.6	15
59	A multi-layered vascular scaffold with symmetrical structure by bi-directional gradient electrospinning. Colloids and Surfaces B: Biointerfaces, 2015, 133, 179-188.	5.0	52
60	Leaky Rectangular Waveguide With Circular Polarization Property. IEEE Transactions on Antennas and Propagation, 2015, 63, 5098-5101.	5.1	10
61	Dexamethasone loaded core–shell SF/PEO nanofibers via green electrospinning reduced endothelial cells inflammatory damage. Colloids and Surfaces B: Biointerfaces, 2015, 126, 561-568.	5.0	56
62	Laccase Biosensor Based on Electrospun Copper/Carbon Composite Nanofibers for Catechol Detection. Sensors, 2014, 14, 3543-3556.	3.8	61
63	Direct electrochemistry of laccase and a hydroquinone biosensing application employing ZnO loaded carbon nanofibers. RSC Advances, 2014, 4, 61831-61840.	3.6	14
64	Amperometric detection of hydrogen peroxide using a nanofibrous membrane sputtered with silver. RSC Advances, 2014, 4, 3857-3863.	3.6	21
65	Novel Phenolic Biosensor Based on a Magnetic Polydopamine-Laccase-Nickel Nanoparticle Loaded Carbon Nanofiber Composite. ACS Applied Materials & Interfaces, 2014, 6, 5144-5151.	8.0	117
66	Laccase Immobilized on a PAN/Adsorbents Composite Nanofibrous Membrane for Catechol Treatment by a Biocatalysis/Adsorption Process. Molecules, 2014, 19, 3376-3388.	3.8	56
67	Thermal and mechanical properties of nanofibers-based form-stable PCMs consisting of glycerol monostearate and polyethylene terephthalate. Journal of Thermal Analysis and Calorimetry, 2013, 114, 101-111.	3.6	18
68	Electrospun form-stable phase change composite nanofibers consisting of capric acid-based binary fatty acid eutectics and polyethylene terephthalate. Fibers and Polymers, 2013, 14, 89-99.	2.1	41
69	Fabrication and characterization of polyamide6-room temperature ionic liquid (PA6-RTIL) composite nanofibers by electrospinning. Fibers and Polymers, 2013, 14, 1614-1619.	2.1	13
70	Reconfigurable Design for Automatic Visual Inspection by Extension Theory. , 2010, , .		0
71	Development of a sensitive and groupâ€specific polyclonal antibodyâ€based enzymeâ€linked immunosorbent assay (ELISA) for detection of malachite green and leucomalachite green in water and fish samples. Journal of the Science of Food and Agriculture, 2009, 89, 2165-2173.	3.5	55
72	A sensitive immunochromatographic assay using colloidal gold–antibody probe for rapid detection of pharmaceutical indomethacin in water samples. Biosensors and Bioelectronics, 2009, 24, 2277-2280.	10.1	73

#	Article	IF	CITATIONS
73	Microwave-Induced Thermal Treatment of Petroleum Hydrocarbon-Contaminated Soil. Soil and Sediment Contamination, 2008, 17, 486-496.	1.9	10
74	Enhanced biodegradation of para-xylene by the marine cryptophyte Rhodomonas sp. JZB-2 by changing the concentrations of nutrients, iron, and vitamins. Journal of Applied Phycology, 0, , .	2.8	2